2008 IEEE International Conference on
Robotics and Automation
Pasadena, CA, USA, May 19-23, 2008

Incorporation of Novel Underwater Thrusters into Vehicle Control Systems

Mike Krieg and Kamran Mohseni

Abstract— **A new type of underwater thruster is studied which is inspired by the natural locomotion of squid and other cephalopod. The thruster is similar to synthetic jet actuators used for flow control studies, but operates on different length and frequency scales. A hybrid simulation experiment has been designed to test the performance of this thruster in a static environment, under dynamic, unsteady driving signals. The hybrid simulation implements actual thrust production on a virtual vehicle model and attempts to control the trajectory of that vehicle. It was determined that this type of thruster being controlled with a basic PD control algorithm demonstrates excellent position tracking in a wide range of maneuvers. The thruster showed that it could produce controlling forces accurately on several scales of thrust. However, the maneuvering system was subject to an appreciable position overshoot at high vehicle oscillation frequencies, due to unmodeled thruster settling time.**

I. INTRODUCTION

Unmanned Underwater Vehicles (UUVs) present an interesting challenge in the field of robotics and automation. The technical challenges and costs of sending humans to the harsh marine environments, in which most of these vehicles operate, practically necessitates a robotic presence; while at the same time all but eliminating long range communication. The open ocean takes our drones far beyond the controlling grasp of their parents; making the depths the perfect testing grounds for adaptive fully autonomous robots.

One of the largest setbacks preventing the development of a sustainable underwater robot is a lack of accurate maneuvering capability. Without a constant human presence the vehicles must have some way of autonomously refueling, transferring data, and updating mission objectives. This would most likely take place at a set of stationary docks or buoys, which serve as power generators and long range communication relays. In addition these stations could easily serve as nodes for a navigational system similar to Long-base-line (LBL) navigation (for a summary of LBL navigation see [1]).

Docking has proven to be a challenge in underwater environments. Low speed underwater maneuvering is almost entirely accomplished by propeller type thrusters and is; therefore, subject to the limitations of this type of propulsion.

This work was supported by a grant from the National Science Foundation (NSF)

Mike Krieg is a graduate student in the Department of Aerospace Engineering at the University of Colorado at Boulder, 429 UCB, Boulder Colorado 80309 michael.krieg@colorado.edu

Kamran Mohseni is an Associate professor of Aerospace Engineering Sciences at the University of Colorado at Boulder, 429 UCB, Boulder Colorado 80309 kamran.mohseni@colorado.edu

An alternative form of propulsion was recently investigated [2] which is inspired by the natural locomotion of squid and other cephalopod. By this method low momentum fluid is ingested into a cavity (known as the mantle for squid), and subsequently ejected with a much higher momentum through an orifice. The high momentum fluid rolls into a vortex ring, and carries the momentum away from the animal. The resulting momentum transfer propels the squid forward. Several generations of thrusters have been built and tested to prove the feasibility of this type of propulsion from an engineering standpoint, and the primary characteristics of this type of thruster were empirically determined ([2]–[4]).

The work described within this manuscript was performed in an attempt to demonstrate the feasibility of using this type of thruster in a dynamic real world environment, by studying its response to a dynamic unsteady driving signal. A basic description of our thruster can be found in Section II. An explanation of a virtual model used to mimic vehicle motion, as well as a description of the experimental setup is given in Section III. Section IV gives a discussion on the characteristic sizing of maneuvers. The virtual vehicle controller design is provided in section V. The performance of our thruster in various operational regimes is given in Section VI

II. THRUSTER DESCRIPTION

As was mentioned in the introduction the actuation cycle for our thruster begins with the ingestion of low momentum fluid into a cavity. The cavity for this device consists of a rigid shallow cylinder with a flexibly plunger within, as is shown in Figure 1. The plunger is made of semi-flexible ducting. The surrounding fluid can be thought of as a perfectly incompressible fluid, so that any deflection of the plunger is linearly proportional to the volume change of the fluid within the cavity.

In the second phase of the actuation the plunger returns to the extended position and ejects a jet into the surrounding fluid. The ejected jet immediately rolls into a vortex ring and carries the high momentum fluid sufficiently far from the thruster. The key parameters which affect the thrust generation are the frequency of actuation, and a geometric parameter of the jet known as the formation ratio, which is the ratio of the length to diameter (L/D) of the jet if it were unaffected by the surrounding fluid (as shown in Figure 1). This device will be called a vortex ring thruster (VRT) throughout the paper.

978-1-4244-1647-9/08/$25.00 ©2008 IEEE.

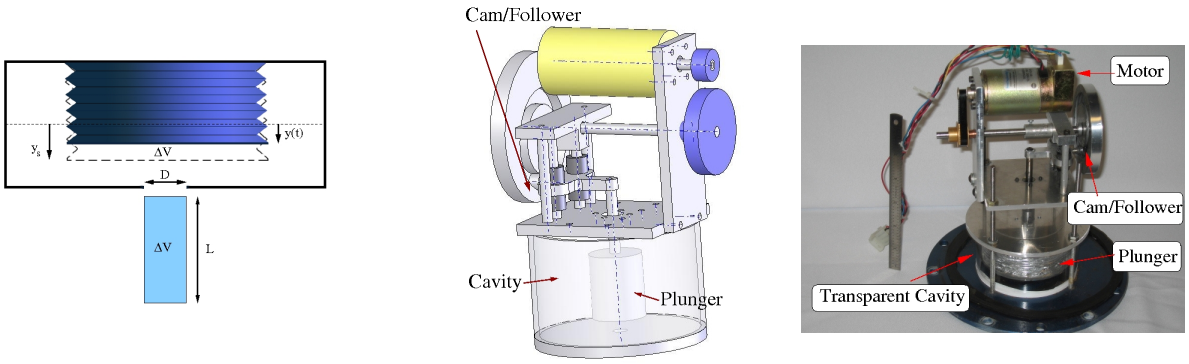

Fig. 1. Vortex Ring Generator: Theoretical Model and Actual Device (a) Conceptual model of the actuator (b) CAD model of the actual device (c) Actual Device.

A. *Thruster Characteristics*

The VRT's dependence on actuation frequency, and formation ration was examined extensively in previous studies [2], [3]. A slug model was developed in these studies to predict the thrust production. The slug model predicted that the thrust produced from a device with a sinusoidal jet ejection velocity profile had a square dependence on the oscillation frequency.

$$\bar{T} = \rho \frac{\pi^3}{16} L^2 D^2 f^2 \tag{1}$$

This thrust prediction was observed to be accurate for the thruster operating at frequencies below the cavitation frequency (critical frequency where fluid within cavity vaporizes due to pressure loss), and below the formation number. The formation number is defined as the maximum formation ratio whereby the entire jet is injected into the vortex ring. Above the formation number the induced velocity of the vortex ring causes it to "pinch-off" of the remaining shear flow and the vorticity of the vortex ring becomes saturated. The formation number was determined by Gharib et. al. [5] to have a universal value of about 4 for all jets studied.

Though these thrusters have been fully characterized with respect to their important actuation parameters, very little is known about their dynamic response in a vehicle environment. This paper will attempt to characterize the response of these thrusters when being controlled by an unsteady input driving signal which is typical of what would be encountered in a dynamic environment.

III. Virtual Model

Due to the abundance of complexities involved with controlling a fully unrestrained vehicle, a simpler method is desired to determine the dynamic performance of a thruster. A method was proposed by Yoerger et al. [6] whereby the behavior of a vehicle was modeled by a system with a single degree of freedom; and the thrust was measured empirically from a controlled static setup. The governing equation for the system is given by the simple drag equation.

$$M\ddot{x} = T - C_D \dot{x} \mid \dot{x} \mid \tag{2}$$

Where, x is the unrestrained axis, M is the mass of the vehicle (including an added mass), T is the force provided by the thruster, and C_d is the coefficient of drag. In [6] this coefficient has been derived from actual vehicle data; in this study however, since there is no actual vehicle to work from, this coefficient will be assumed to be the drag coefficient for a cylinder in laminar cross flow. This assumption seems appropriate since the primary uses of these thrusters are for maneuvers involving rotation and sideways translation, both of which induce a cylinder cross flow.

The virtual model assumes that the vehicle starts at rest. At the onset of the experiment the vehicle is assigned a desired trajectory or mission objective. A control algorithm, which will be discussed later, determines an appropriate control force and sends a signal to drive the VRT. The corresponding force from the thruster is measured using a load cell. The thrust is then fed into the virtual algorithm, and the vehicle motion is integrated according to equation (2). In real time the control algorithm attempts to control the virtual vehicle using the actual forces generated by the thruster within its test environment. A functional block diagram of this system is shown in figure 2.

Of course this simple drag model ignores many of the key parameters which would affect the operation of an actual vehicle with this type of thruster; most notably the affect the surrounding flow will have on the thrusters. It was determined by Krueger et. al. [7] that jets produced in the presence of a background co-flow will experience "pinch-off" at a lower stroke ratio, as the flow velocity approaches the jet velocity. Since a moving vehicle will experience a cross flow the effects of co-flow on thrust should not be dismissed, but are difficult to model in a virtual environment. In spite of the simplicity of the model, it allows for the performance of the thruster to be observed much more easily without the arduous process of construction of an actual vehicle.

The water tank, which houses the fluid reservoir, was designed and fabricated by our group specifically for this investigation. It is 7' tall, and 3' by 4' in cross section and houses 700 gallons of water. The tank is made out of acrylic to allow for visual access from all angles (including

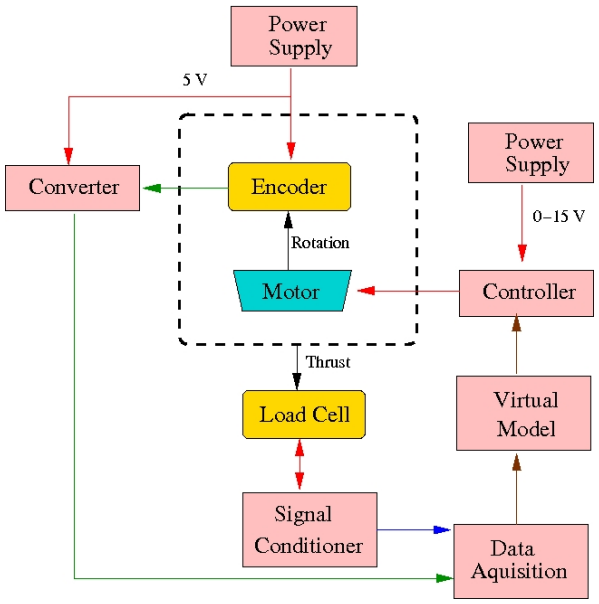

Fig. 2. Testing Setup Functional Block diagram.

Fig. 3. Actuator Testing Tank.

the bottom of the tank), and is supported by an outer steel skeleton. At the top of the tank is a mounting structure which is securely attached to the outer frame. This mounting structure contains of a set of linear bearings which restrict the actuator's lateral motion, while allowing the axial thrust to be translated through the connecting rod to the force sensor. Also contained on the mounting structure is a mounting bracket which holds our force sensor and provides a rigid constraint for proper sensor measurement. The tank with the actuator mounted inside is depicted in Figure 3.

The thrust is measured directly using a PCB 1102 load cell canister. The virtual model only integrates at a rate of 100 Hz due to software/processing limitations. This is much too slow to capture the dynamic nature of the thrust. As a result the thrust is sampled at a rate of 10000 Hz, and an average is calculated every 100 samples which is used as the thrust value during the integration.

IV. Maneuver Scaling

The ultimate goal of this type of maneuvering technology is to achieve a high accuracy loiter or hover, so that the vehicle can engage some docking mechanism and perform autonomous upkeep. Marine environments are cluttered with wave like current disturbances. To overcome these disturbances a vehicle must provide a wide range of controlling forces. Constructing a virtual wavelike disturbance, for the maneuvering system to overcome, would be complicated and would most likely constitute a poor representation of actual marine disturbances. Instead this experiment will attempt to track a position reference with the virtual vehicle in a quiescent fluid environment. Any arbitrary desired trajectory can be decomposed into a fourier set of sinusoidal trajectories. Though the non-linearities of our system prevents the ability to superimpose the set of simple trajectories on each other to realize the desired trajectory, they still require forcing which is indicative of what would be required for the ultimate desired trajectory. Therefore, this experiment will attempt to drive the thruster to provide controlling forces necessary for trajectory reference tracking over a set of basic sinusoidal maneuvers. This way appropriate control algorithms and parameters may be determined. These basic maneuvers will take on the form

$$x(t) = A\sin(2\pi f t) \tag{3}$$

Where A is the amplitude of the maneuver, and f is the frequency of oscillation. Though these parameters appear arbitrary they can be defined intrinsically to a characteristic sizing.

Typically the parameters defining the extent of maneuvers would be defined in terms of actual vehicle requirements. This presents a problem in the absence of an actual vehicle architecture. The solution presented within this manuscript is to define optimal vehicle parameters with respect to thruster capabilities, and to restrict the maneuvering parameters accordingly. In essence, to define a vehicle for which the thruster of this investigation would be ideally suited and to define typical maneuvers for such a vehicle.

Consider again that the virtual model assumes the vehicle to be a perfect cylinder. The characteristic size of that cylinder is the diameter. If all vehicles are assumed to have the same aspect ratio (denoted here by σ), then the geometry is reduced to the diameter d. The limitation on the thruster

is the maximum thrust it can produce while still being accurately described by the slug model of [2]; this thrust will be denoted T_m. If a thruster bounded by T_m is operating on a vehicle of mass M, the maximum acceleration it can attain can be derived from the drag equation assuming there is no forward velocity (which is just Newton's second law).

$$\ddot{x_m} = \frac{T_m}{M} \tag{4}$$

Assuming that a vehicle is designed to be close to neutral buoyancy, the mass of the vehicle can be easily described in terms of the characteristic geometry; $M = \frac{\pi\rho\sigma}{4}d^3$, where ρ is the fluid density and the rest of the terms are consistent with previous notation.

Additionally, if the vehicle is to perform a maneuver of the form described in equation (3) then the maximum acceleration required throughout the entire maneuver is $\ddot{x}_{max} = 4\pi^2 f^2 A$. The maximum vehicle acceleration and maximum maneuver acceleration should be closely related in any design. η is defined to be the ratio of the maximum maneuver acceleration to the maximum attainable vehicle acceleration. For this experiment this ratio was set to 75%. After a little algebra the maneuver frequency can be defined in terms of the thrust and maneuvering amplitude A. Again the maneuvering amplitude is arbitrary, the ratio of the maneuver amplitude to the vehicle size is much more indicative of the mission. If this ratio is defined by $A^\star = A/d$ the frequency can be determined with respect to the characteristic sizing.

$$f = C \cdot \sqrt{\frac{T_m}{A^\star}}\frac{1}{d^2}, \quad C = \sqrt{\frac{\eta}{\rho\sigma\pi^3}} \tag{5}$$

In this sense the maneuvering frequency is not arbitrary but dependent upon the characteristic geometry defined by d, the thruster capacity defined by T_m, and the ratio of the maneuvering amplitude to the characteristic geometry. This ratio should be thought of as a maneuvering regime. Maneuvers with amplitudes much larger than the characteristic geometry are in the *transit regime* moving a vehicle to its sight of interest. Maneuvers which are much smaller than the characteristic geometry are in the *docking regime*, these maneuvers require a high accuracy, and fast tracking.

The VRT's performance will be tested in 3 regimes to demonstrate a high versatility. These regimes will have amplitude to geometry ratios with values of $A^\star = 2$, $A^\star = 0.1$, and $A^\star = 0.05$.

V. Controller Architecture

A virtual model has been fully defined capable of predicting vehicle motion given thrust measurement inputs. In addition a set of specific characteristic maneuvers has been defined with respect to vehicle parameters. Now a controller must be implemented on the thruster to close the control loop and drive the virtual vehicle along the desired trajectory. The VRT is a completely new style of thruster, and as such there is little understanding of how it will perform in a dynamic vehicle environment (in fact this type of thruster has only been successfully installed on one vehicle).

Given the lack of practical experience with VRT's in vehicle environments the thruster controller is first set to be a simple proportional derivative controller with a feed forward term to compensate for drag forces. Operating the thruster with this basic control algorithm will demonstrate parameters of the thruster which require controller compensation. This controller determines a desired control force u according to

$$u = K_p\tilde{x} + K_d\dot{\tilde{x}} - Cd\dot{x} \mid \dot{x} \mid \tag{6}$$

where $\tilde{x}$ is the error between the vehicle's desired position and its actual position $\tilde{x} = x_d - x$, likewise, $\dot{\tilde{x}}$ is the error between the desired and actual vehicle velocities, K_p is the proportional gain constant, and K_d is the derivative gain constant. The values of the proportional and derivative gain terms were set arbitrarily during experimentation to achieve sufficient controller performance. For all the maneuvers examined within this paper both gains were set to 20. The additional term in the equation is a term which compensates for the drag forces which are already acting on the vehicle when the control action is taken.

When the controller determines an adequate control force, it must be related to the thruster controlling parameters to be realized. Equation (1) tells that the thruster force output is proportional to the square of the actuation frequency. If this equation is rearranged it gives an equation for the desired driving frequency based on the desired control force, and the thruster operational parameters.

$$f = \sqrt{\frac{16u}{\rho\pi^3 L^2 D^2}} \tag{7}$$

This frequency is controlled using an external motor controller (AMC BE15A8 servo amplifier). This way the dynamics of the motor could be ignored in the vehicle controller since the motor drive system is not inherent to the vortex ring thruster.

VI. Results

The performance of the thruster will first be analyzed for the case of maneuvers in the transit regime. Again this regime is characterized by vehicle maneuvers which are sufficiently larger than the vehicle characteristic geometry.

It can be seen from Figure 4 that the VRT has excellent tracking characteristics with respect to the vehicle trajectory in the transit regime. There is a small deviation between the desired and actual motion at the onset of the maneuver. This error is due to the fact that, even though the vehicle and desired maneuver start from the same position, they start from very different velocities. The acceleration needed to bring the vehicle to the maneuvers initial velocity instantaneously is not accounted for in the scaling of the maneuver and is well outside the range of the acceleration achievable with the thruster. However, once this initial velocity discrepancy was overcome, the thruster was able to maintain a vehicle trajectory almost identical to the desired trajectory.

Now consider the vehicle performing a maneuver in the docking regime. This regime is characterized by vehicle

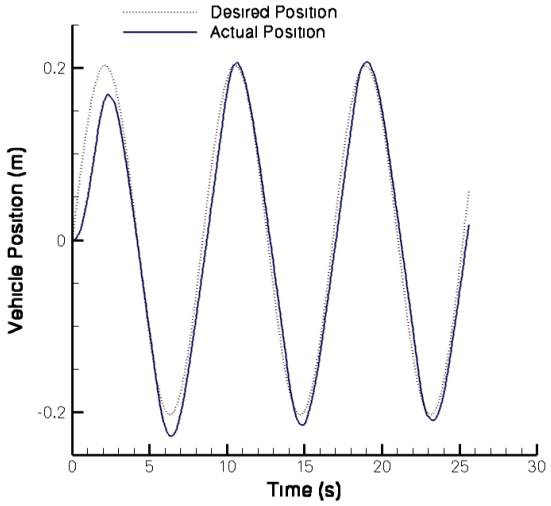

Fig. 4. The desired and actual trajectories of the virtual vehicle in the transit regime

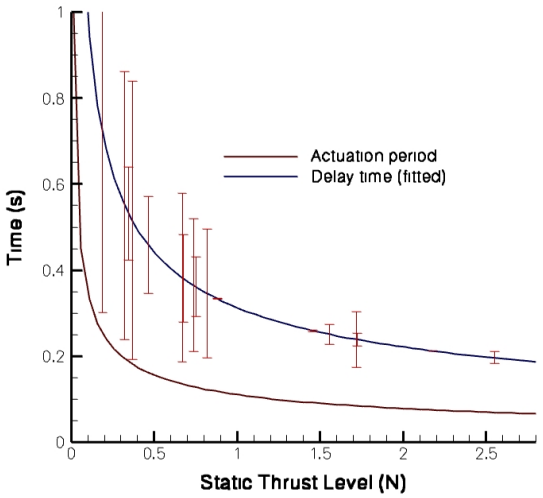

Fig. 6. Thrust settling time as a function of thrust level

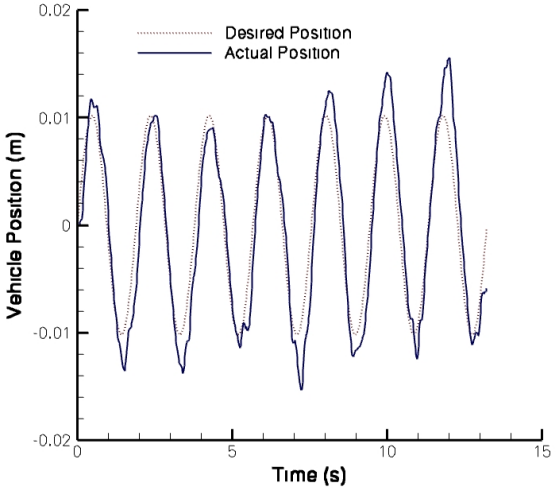

Fig. 5. The desired and actual trajectories of the virtual vehicle in the docking regime

maneuvers which are orders of magnitude smaller than the vehicle characteristic geometry.

Figure 5 demonstrates that the thruster was able to accurately control the motion of the vehicle on a much smaller scale. The initial lack of tracking performance seen in the transit regime is not present in this smaller regime; due to the fact that the smaller amplitude results in a lower initial velocity, keeping the initial acceleration within the limits of the thruster. Another difference which can be seen in the docking regime is a small overshoot at the edge of the maneuver. This is due to the fact that at these locations the level of thrust must change magnitude and direction rapidly.

Equation (1) fully describes the thrust generated for a VRT operating at various conditions, but it completely ignores the manner in which the thruster reaches that level of thrust. There is a time delay associated with the thruster settling on the thrust predicted by equation (1). Similar to propellor type thrusters [6], the VRT has time delays which are inversely proportional to the desired level of thrust. A characteristic time scale for the thruster is the period of a single pulsation, which is proportional to the inverse of the square of the thrust. Therefore, the time delay will be assumed to take on the same proportionality.

$$t_{delay} = \frac{a}{\sqrt{T}} \tag{8}$$

Several sets of data were analyzed to determine the functionality between the time delay and the level of thrust. The settling times were then fit to a curve of the form described in equation (8). This curve, along with the characteristic pulsation time is shown in Figure 6. This particular fitted curve has a proportionality constant of $a = 0.313$

As can be seen from Figure 6 the time delay demonstrates a similarity to the characteristic pulsation time. The errorbars show a strong agreement for the time delay of larger thrust values, but a great degree of scatter in the lower thrust ranges. This scatter is mostly a measurement error which comes from two sources. First, the thrust signal from the VRT is extremely dynamic (from the oscillatory nature of the jet), which makes the determination of the static value non-trivial. As the thrust level decreases along with the actuation frequency, it becomes exceedingly difficult to determine the static component of thrust in such as small range of data. Noise in the signal subsequently has a greater effect on the determination of t_{delay}. In addition the fact that the level of the total thrust is so much lower, causes the noise to again have a much greater response on the determination of t_{delay}.

The fact that this time delay associated with reaching desired forces is unmodeled in the basic control law of 6 is the cause of the overshoot seen in the docking regime. If

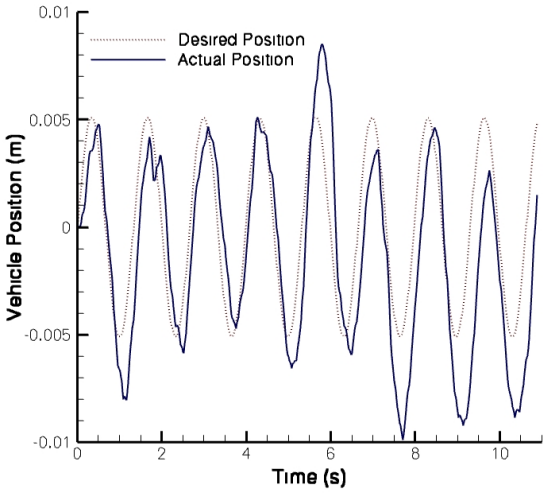

Fig. 7. The desired and actual trajectories of the virtual vehicle in the reduced docking regime

the scale of the maneuver is reduced even further ($A^\star = .05$), this consequence can be seen more drastically.

When the scale of the maneuver is decreased, the frequency of vehicle oscillation is also increased. Even though the maximum acceleration required to oscillate at that frequency is maintained at a constant level, the lag associated with thruster settling makes such high frequency maneuvers impossible without further controller compensation, although it should be noted given the small scale of the maneuver, the overshoot may be below the required resolution of the maneuver for docking.

It should also be noted that the scale of the thruster can, hypothetically, be adjusted during the mission to eliminate the overshoot seen in figure 7. This could not be performed with the test thruster used in this experiment because the plunger driving mechanism was fixed mechanically; however, if the driving mechanism was electrically operated (solenoid, voice coil, etc.) the stroke length could be adjusted during operation. This means that the max thrust given in equation (4) can be reduced during operation. This will allow the thruster to reduce the time delay for any given thrust, and avoid the overshoot seen in the *docking regime* without introducing a more complicated control architecture.

Despite the fact that the trajectory reference tracking of our simple controller system is subject to overshoot in the small *docking regime*, the trajectory of the vehicle is still smooth and absent of small scale waves. The lack of small scale thruster dynamics supports the claim made in [2] that the level of thrust produced by a VRT is quantizable down to the level of a single jet pulsation, which is well below the resolution of a typical vehicle position determination system.

VII. CONCLUSIONS AND FUTURE WORKS

A virtual model of an underwater vehicle with a single degree of freedom was constructed (including a simplistic drag estimation). Using this model, thrust measured from an experimental thruster in a static environment was numerically integrated to predict resulting vehicle motion. A basic PD controller was constructed to control the thuster driving the vehicle along predefined desired trajectories. Using this hybrid simulation, the performance of a new vortex ring thruster in with unsteady driving signals was observed. The system was determined to have excellent position tracking in the large scale transit maneuvers, but suffered from a high degree of overshoot in the small scale parking maneuvers due to the unmodeled thrust settling time of the thruster.

Given the overshoot seen in the very small maneuvering regimes, future experiments will be conducted where the simple PD controller is expanded to include both a lead compensator and a sliding controller compensator. In addition a new physical vehicle test bed is currently under construction which will allow the thrusters to be tested in a true dynamic environment. The results of this study will be used in designing vehicle missions, to prove the effectiveness of these thrusters in specific maneuvering regimes.

VIII. ACKNOWLEDGMENTS

Special thanks to Advanced Motion Control, for providing a high power servo amplifier at no cost which was used to control motor frequency. Thanks are also extended to Prof. Eric Frew for his help in the editing of this manuscript.

REFERENCES

[1] J. Bellingham, "New oceanagraphic uses of autonomous underwater vehicles," *Marine Technology Society journal*, vol. 31, no. 3, pp. 34–47, 1997.

[2] M. Krieg and K. Mohseni, "Thrust characterization of a bio-inspired vortex ring thruster for locomotion of underwater robots," *Journal of Ocean Engineering*, vol. Accepted, 2008.

[3] K. Mohseni, "Pulsatile jets for unmanned underwater maneuvering," Chicago, Illinois, AIAA paper 2004-6386, 20-23 September 2004, 3rd AIAA Unmanned Unlimited Technical Conference, Workshop and Exhibit.

[4] A. Polsenberg-Thomas, J. Burdick, and K. Mohseni, "An experimental study of voice-coil driven synthetic jet propulsion for underwater vehicles," in *Proceedings of the OCEANS 2005*. Washington, D.C.: MTS/IEEE, September 19-23 2005.

[5] M. Gharib, E. Rambod, and K. Shariff, "A universal time scale for vortex ring formation," *J. Fluid Mech*, vol. 360, pp. 121–140, 1998.

[6] D. Yoerger, J. Cooke, and J.-J. Slotine, "The influence of thruster dynamics on underwater vehicle behavior and their incorporation into control system design," *IEEE Journal of Oceanic Engineering*, vol. 15, no. 3, pp. 167–178, 1990.

[7] P. Krueger, J. Dabiri, and M. Gharib, "The formation number of vortex rings formed in a uniform background co-flow," *Journal of Fluid Mechanics*, vol. 556, no. 1, pp. 147–166, 2006.